JOURNAL OF MATERIALS SCIENCE **38** (2003) 2525–2536

Relevance of roughness parameters for describing and modelling machined surfaces

M. BIGERELLE, D. NAJJAR, A. IOST
Laboratoire de Mètallurgie Physique et Gènie des Matèriaux, UMR CNRS 8517, Equipe Surfaces et Interfaces, Ecole Nationale Supèrieure d'Arts et Mètiers, 8 Boulevard Louis XIV, F59046 Lille Cedex, France
E-mail: denis.najjar@lille.ensam.fr

Describing and modelling a machined surface require the selection of relevant roughness parameters. However, this selection is difficult since a machined surface morphology can be described by a large number of roughness parameters.

This investigation focuses on the roughness of metallic surfaces taking for two applications: a) the description of machined surface morphologies produced by grinding b) the relationships between machined surface morphologies (grinding or cold-rolling) and their brightness level when irradiated by the white light beam of an optical glossmeter used for industrial surface quality control. For each application, the aim is to determine, from an objective quantitative point of view, the relevance of one hundred or so surface roughness parameters. To reach this objective, a specific software program has been developed to determine a ranking of relevance thanks to the calculation of a computed statistical index of performance.

The statistical results of this study show that the fractal dimension estimated by an original method is the most relevant roughness parameter to describe the surface morphology after grinding or rolling. Because of this relevance, this roughness parameter has also to be taken into consideration in models showing the interactions between machined surfaces and an optical wave. The methodology presented in this study can be a useful tool in the quality control phase to keep under control the fabrication process parameters of manufactured objects in industrial environments.

1. Introduction

The precise characterization of roughness is of prime importance in many engineering industries because of its considerable influence on the functional properties of machined surfaces. Specific cases are: a) sliding counterfaces when friction is concerned ii) rolled steel sheets that must undergo a subsequent surface treatment like galvanizing or chromium plating iii) polished surfaces that must present a high degree of reflectivity ....

As costs have to be minimized, manufacturers aim to develop reliable control methodologies suitable for use in routine production environments. These control methodologies must be simple, quantitative with a high degree of repeatability [1].

The topographic methods are by far the most widely used in the surface quality assessment of metallurgical or mechanical products. The most commonly used and cheapest devices are contact profilometers that are very accurate but not suitable for in-process measurements as they have to be brought into contact with the surface of the workpiece. That is why optical techniques have been developed to substitute traditional contact profilometry in surface quality control [1–5].

In an industrial environment and in research laboratories, it is common to quantify surface morphology in terms of roughness parameters such as the arithmetic average roughness R_a, root-mean square roughness R_q, peak-to-valley roughness R_t or number of peaks per inch N_p. Such roughness parameters are estimated to qualify the surface quality of the products. Simultaneously, scientists have mainly developed two kinds of models to describe rough surfaces [6]: one is the deterministic model and the other is the stochastic model that takes into consideration the correlation length L_{ac} of the surface. However, machined surfaces are rarely purely periodic or truly random, that is why the fractal concept first introduced by Mandelbrot [7–15] has been much worked upon to characterize these more complicated surface morphologies.

Still, we might wonder which of the various parameters is the most relevant one to characterize the morphology of a machined surface with regard to a specific application (an optical quality control for example). The main purpose of this investigation is to propose a methodology in order to answer this question without any preconception on the possible relevance of any roughness parameter. Thus, only a statistical approach

using intensive computer calculations seems appropriate to treat the experimental data in our opinion.

To the authors' knowledge, the usual software programs available on the market present numerous limits and are particularly inadequate for statistical analysis. Indeed, they are often developed in combination with a specific measurement device and allow the estimation of few surface roughness parameters from only one data file. A specific software program that both avoids the above cited problems and answers the previous question was developed and tested to study the relevance of one hundred or so surface parameters for two applications on metallic materials: a) the description of machined surface morphologies produced by grinding b) the relationships between machined surface morphologies (grinding or cold-rolling) and their brightness level when irradiated by the white light beam of an optical glossmeter.

2. Materials and experimental procedure

2.1. Presentation of materials

Two pure metals, aluminum and copper, and two alloys, an industrial low carbon steel Fe-0.05%C and a tin alloy Sn-5%Sb, have been chosen to study the machined surface morphologies produced by grinding and their relationships with an optical wave. These materials have been selected because of their different microstructures, mechanical and optical properties in order to emphasize the reliability of the statistical results of this study. General characteristics of these materials are reported in Table I.

It must be added that, in the case of the industrial low carbon steel, the as-received material surface morphology was obtained by cold rolling since this material was manufactured for specific applications requiring a bright finish aspect. The cold rolling process included a 4 stand tandem mill and a temper mill (skin-pass) that induced high and low surface roughness values respectively.

2.2. Presentation of experimental procedure

2.2.1. Measurements

Two samples of $40 \times 40\ mm^2$ area were ground for each material at grade 80, 120, 220, 500, 800, 1000, 1200 and 4000 (number of grains per cm^2) using an automatic grinding machine with abrasive SiC papers. This grinding process, performed under similar experimental conditions (grinding time = 90 s and pressure = 2.3 10^4 Pa) in each case, leads to typical surface morphologies with an isotropic texture (at the eye scale) consisting of randomly distributed scratches. However, the values of the roughness parameters characterizing these surface morphologies were different since they depend on the mechanical properties of the material and the paper grade.

For each sample and paper grade, fifteen profiles have been recorded at random with a tactile profilometer Perthen. This device consists of a diamond tip with a 5 μm rounded-end. For each measurement, the stylus was moved linearly across the surface under a 0.8 mN load at a constant speed of 1 $mm \cdot s^{-1}$. This device records and electrically amplifies approximately 8000 points along the tracing length (equal to 1 mm for this study) to characterize the vertical movements of the stylus relatively to the horizontal one. According to the manufacturer, the vertical stroke of the stylus is 200 μm with a 15 bit digital resolution corresponding to a 0.006 μm vertical resolution.

Fig. 1 shows profiles and the associated histogram of profiles' heights for grades 80, 220, 1000, 4000. Firstly, note the magnification of the vertical scale relatively to the horizontal one for each profile, and secondly, that approximately 240000 points ($8000 \times 2 \times 15$) have been used to plot the histograms. All the histograms approach the Gaussian distribution.

For each sample and paper grade, fifteen brightness measurements were also recorded at random with a monoangle glossmeter in agreement with the ASTM D523, DIN 67530 and ISO 2813 specifications. Such a device is based on the idea of measuring the specular amount of reflected light directed to a surface at a specified angle from perpendicular. The monoangle glossmeter used in this study casts a white light beam at a 60° incidence angle and a detector records the amount of reflected intensity in the specular (mirror) direction. The amount of light reflected from the surface, that is to say the brightness level (or the specular gloss as named in the specifications cited above), can be read on the glossmeter screen.

To study the effect of the machining process, the same procedure has been also performed on the as-received cold-rolled samples in the case of the industrial low carbon steel. These samples were taken on-line after the 4 stand tandem mill and after the skin pass mill; the roughness profiles and the brightness level measurements have been recorded perpendicularly to the rolling direction.

2.2.2. Numerical treatment by a specific software program

For the numerical treatment, the recorded profiles have been unfiltered before analysis was carried out. A specific software program has been developed using a statistical approach to simultaneously treat numerous data files gathered in a data base and to estimate numerous profile parameters. Moreover, this software program can quantitatively determine the relative relevance of the associated surface parameters with regard to a physical phenomenon without preconception. This last condition has required the preliminary mathematical definition of statistical performance indexes. For each profile, our specific software program can estimate one

TABLE I Main characteristics of studied materials

Materials	Vickers hardness	Structure
Aluminum (Al)	40	Single phased
Copper (Cu)	100	Single phased
Steel (Fe-0.05%C)	125	Single phased
Tin alloy (Sn-5%Sb)	10	Biphased

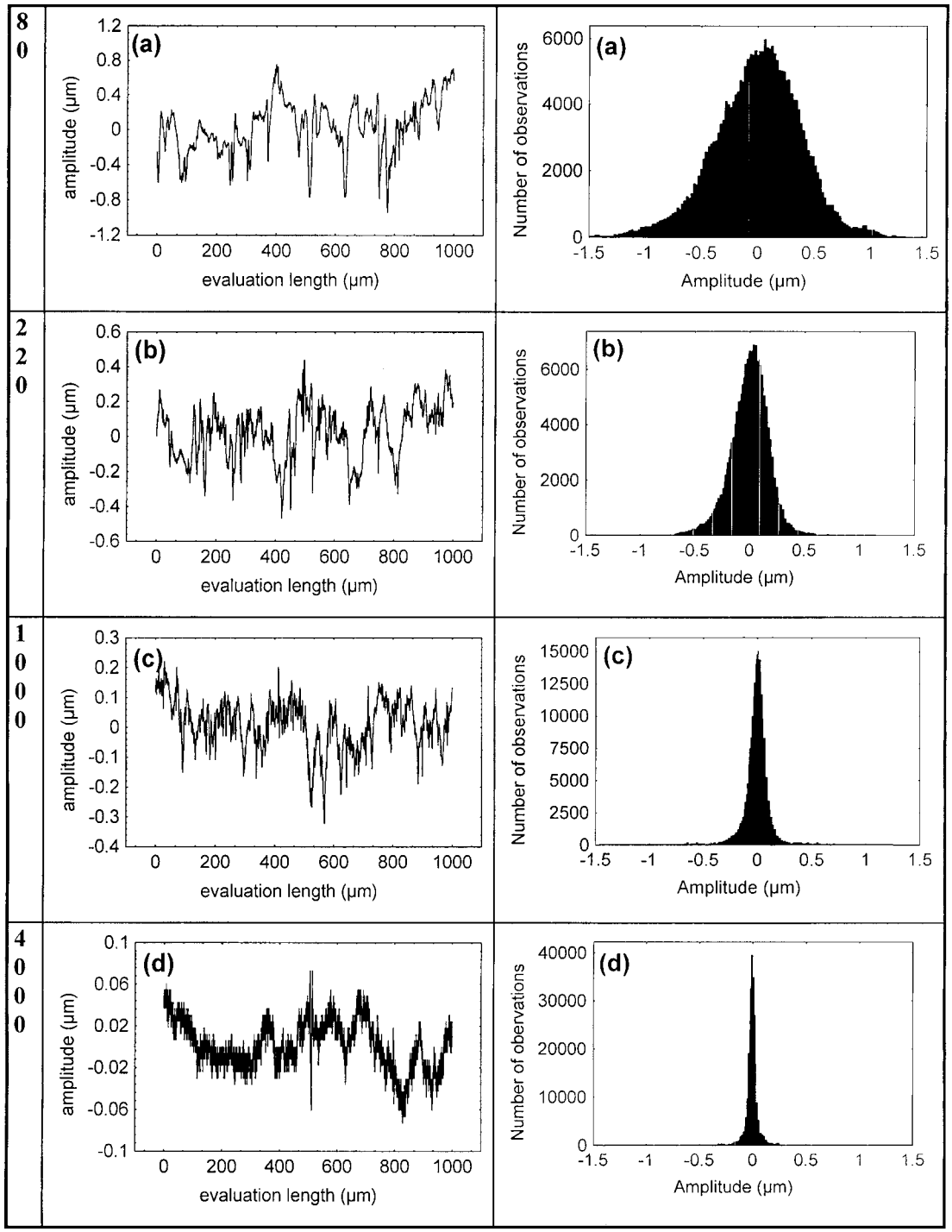

Figure 1 Typical surface profiles and their associated probability histogram of surface height for grades (a) 80, (b) 220, (c) 1000 and (d) 4000. For each grade, the histogram of profile's heights was plotted from approximately 240000 points (8000 × 2 × 15).

hundred or so roughness parameters. In this study particular attention has been paid to the commonly used amplitude and frequency parameters (R_a, R_q, N_p and L_{ac}) and also fractal parameters estimated by different methods. For more details on the other calculated roughness parameters, see [16].

The preliminary mathematical definition of performance indexes has been based on the combination of conventional statistical theories with a more recent powerful one: the Bootstrap theory [17–20]. These indexes, noted F and P, have been defined to correlate the surface parameters with the abrasive wear damage due to the grinding paper grade and with the brightness level respectively.

The index F was derived from the Treatment Index defined in the variance analysis theory briefly summarized in Appendix A [21]. However, this conventional statistical theory does not take into consideration the fact that a small variation in any score influences the vlaue of the Treatment Index. That is why the variance analysis was combined with the Bootstrap theory briefly summarized in Appendix B. The aim of this recent statistical method is to generate N ($N > 500$) equivalent computational sets of data by drawing lots and throwing-in from the set of the experimental values of a given surface roughness parameter i. Then, for each roughness parameter i, a set of N values of F_{ik} ($k \in [1, N]$) can be obtained from which an average

value F_i can be extracted and a 95% confidence interval can be built. From a statistical point of view, a surface roughness parameter i will be more relevant than a parameter j when $F_i > F_j$.

The second index P was defined to correlate the surface parameters with the surface brightness level. As far as the second index P is concerned, the conventional statistical theory used was the linear correlation analysis. To study the relationships between the surface roughness parameters and the brightness level, the main problem to be solved could be summarized as follows: how to correlate a roughness parameter with brightness level when X roughness measurements and Y brightness measurements are made separately on each sample at different points?

The most common alternative is to search for a possible correlation between roughness parameters and brightness level means. However, brightness and roughness experimental variations are lost when using this method and an eventual correlation between them might then wrongly be rejected. The Bootstrap theory can be used again in this case to consider the influence of experimental variations on the estimation of the means. In this case, $N(N > 500)$ equivalent computational sets of data are generated from the experimental set of data associated with each paper grade; each of them thus includes X roughness parameter and Y brightness level values. For each paper grade and each newly generated set of data, both the means of the roughness parameter and the brightness level values can be estimated and a slope value can then be determined if a linear tendency (for example) is expected. For each parameter i, N tendency coefficient values can thus be obtained to a Probability Density Function (PDF) and an unscaled statistical parameter called the Power Correlation P_i can be defined as follows:

$$P_i = \left| \frac{\mu_i}{\sup_i^{97.5\%} - \inf_i^{2.5\%}} \right| \quad (1)$$

where μ_i is the mean of the bootstrapped tendency coefficients and $\sup_i^{97.5\%} - \inf_i^{2.5\%}$ is the 95% interquantile of the bootstrapped PDF that represents the confidence interval.

If $\sup_i^{97.5\%} > 0$ and $\inf_i^{2.5\%} < 0$, that is to say if μ_i approximates the Null value, then there is no correlation between the considered roughness parameter i and the brightness level. When two parameters are significant, the parameter i will be more relevant than the parameter j when $P_i > P_j$ from a statistical point of view.

The most important idea to remember is that, whatever the statistical indexes of performance F_i or P_i, the higher their values, the more relevant the associated surface roughness parameter.

3. Experimental results

3.1. Relevance of surface parameters with regard to the abrasive wear damage due to grinding

Fig. 2 represents the influence of paper grade on the values of the main roughness parameters kept in this study.

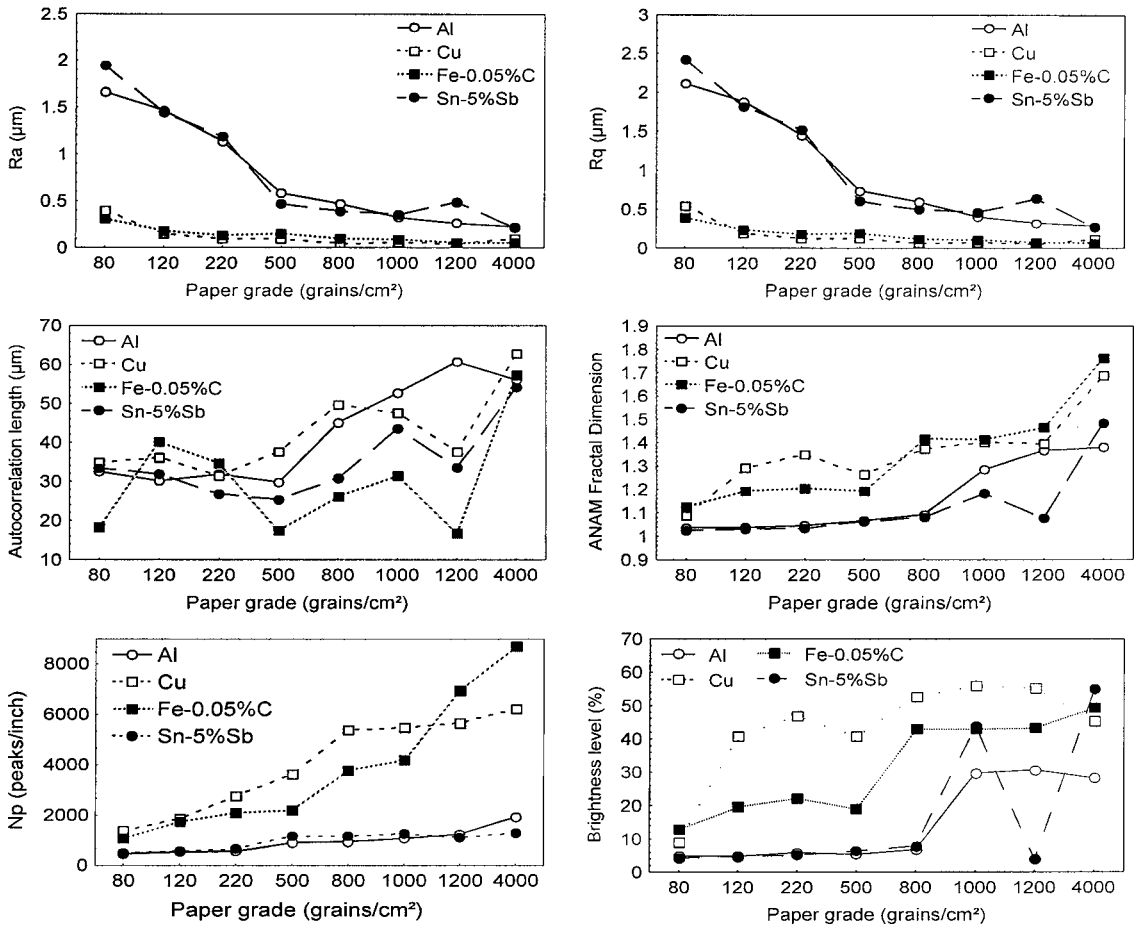

Figure 2 Influence of paper grade on the evolution of R_a, R_q, L_{ac}, N_p, Δ_{ANAM} and brightness level for all ground materials.

The roughness parameter noted Δ_{ANAM} corresponds to the fractal dimension of the experimental profiles estimated by a new method called ANAM (Average Normalized Autocorrelation Method) and developed by the authors [22, 23]. This method, based on the properties of the semi-norm functions L_α, is derived from the Oscillation theory introduced by Dubuc *et al.* [24] and it generalizes the Structure function commonly used in roughness studies.

This new method assumes that the function investigated $z = f(x)$ must be both Hölderian and anti-Hölderian to be applied. However, it does not have to be self-affine contrary to the power spectrum method which is the most commonly used to calculate the fractal dimension of a roughness profile [13, 24]. Briefly, the ANAM consists in evaluating numerically a function noted $K_\tau^\alpha(f, x)$ and formally defined as follows:

$$K_\tau^\alpha(f, L) = \frac{1}{L}\int_{x=0}^{x=L}\left[\frac{1}{\tau^2}\int_{t_1=0}^{\tau}\int_{t_2=0}^{\tau}|f(x+t_1) - f(x-t_2)|^\alpha \mathrm{d}t_1\mathrm{d}t_2\right]^{\frac{1}{\alpha}}\mathrm{d}x \quad (2)$$

where $f(x)$ represents the value of the studied curve profile at the position x, L is the tracing length, τ is the width of a moving window and $\alpha > 1$ is the order of the function.

With the ANAM, the fractal dimension is given by:

$$\Delta_{ANAM}(f, L) = \lim_{\tau\to 0}\left(2 - \frac{\log K_\tau^\alpha(f, L)}{\log \tau}\right) \quad (3)$$

The value of the fractal dimension is then obtained by using the linear regression method to estimate the slope of the plot presenting the variation of $\log K_\tau^\alpha(f, L)$ versus $\log(\tau)$; this slope equals $2 - \Delta_{ANAM}(f, L)$. Fig. 3 shows an example of the plots obtained in the case of the low carbon steel for the different paper grades. It is clear on this graph that there is a linear relationship whatever the paper grade. No crossover, as for example the smooth-rough crossover defined in the new ASME/ANSI B46 [25] and described by Brown *et al.* [26, 27], can be detected on these plots for our experimental conditions. This systematic verification guarantees that the fractal dimension has been estimated without artifact in the fractal regime for each plot.

Fig. 4 is a typical graph, which presents, for the low carbon steel, the values of statistical index of performance F for one hundred or so surface roughness parameters. The information regarding the ranking of

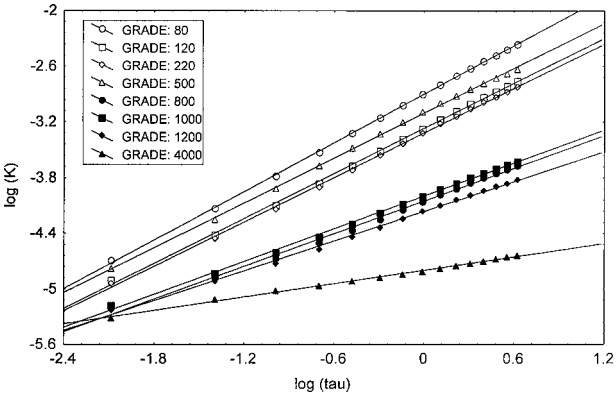

Figure 3 Evolution of the function $\log K_\tau^{\alpha=2}(f, L)$ versus $\log(\tau)$ for the different paper grades in the case of the low carbon steel. For each paper grade the slope equals $2 - \Delta_{ANAM}(f, L)$.

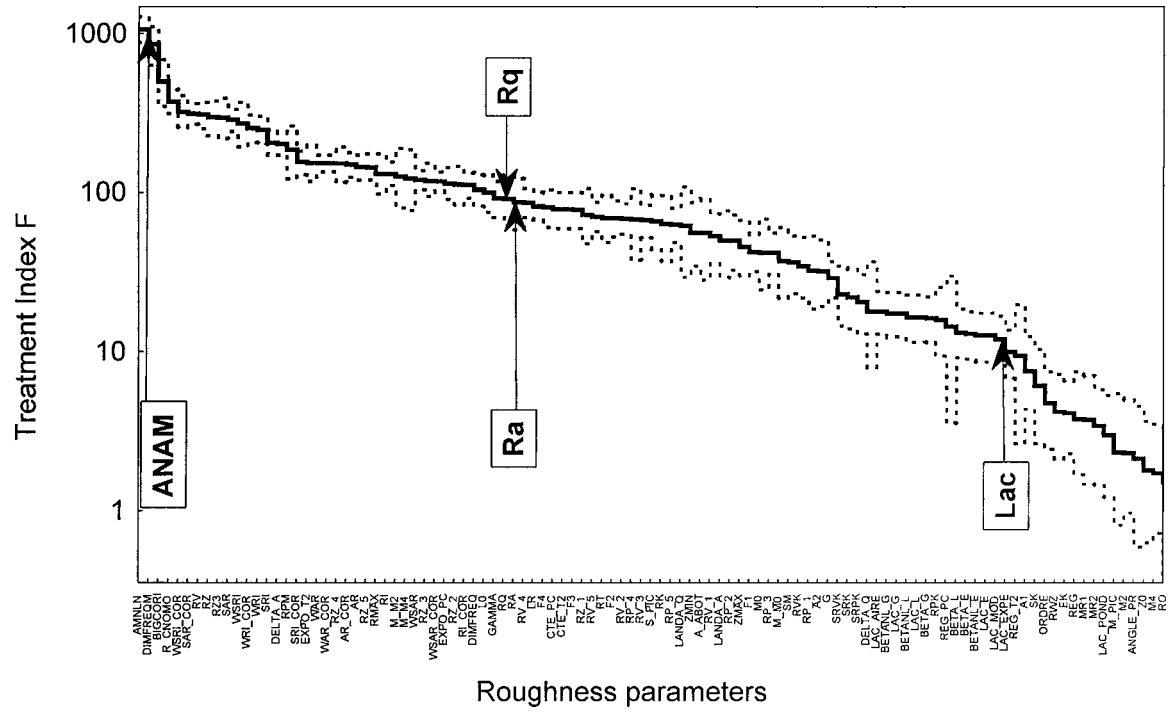

Figure 4 Results of the Bootstrap variance analysis for the ground low carbon steel Fe-0.05%C. Relative roughness parameter ranking according to the value of the statistical index of performance F. The dotted curves represent the 95% confidence level and the straight horizontal line the critical value of F under which the surface roughness parameter can be considered as not relevant.

TABLE II Ranking of the relevant parameters of this study with regards to the paper grade for all tested materials according to the statistical index of performance F (Bootstrap Variance Analysis)

Parameters	Al	Cu	Fe-0.05%C	Sn-5%Sb
R_a	10	31	39	8
R_q (σ)	8	25	38	6
LAC_EXPE (L_{ac})	74	89	89	64
DIMFREQ (Δ_s)	85	62	35	89
ANAMLN (Δ_{ANAM})	1	10	1	1

the relevant parameters of this study is summarized in Table II for all ground materials.

Looking simultaneously at Fig. 2 and Table II, it is clear that commonly used surface parameters R_a and R_q are significantly and similarly relevant with regard to paper grade for soft materials (HV $<$ 50) whereas they are significantly less relevant for hardest ones (HV $>$ 100). Whatever the material, the correlation length L_{ac} is by far the least relevant parameter among those to which a particular attention has been paid in this investigation.

Even if R_a and R_q are relevant parameters, they only rank 8th and 6th positions in the best cases. That is to say that these parameters are not the most relevant ones with regard to the abrasive damage due to grinding.

As to the fractal dimension, it can be seen that the result of its estimation is less relevant using the power spectrum method (Δ_s) [13, 24] than the ANAM one (Δ_{ANAM}). The fractal dimension estimated by the ANAM is always more relevant than R_a and R_q. Except for copper (10th position), this parameter always ranks in first position.

Since the fractal dimension estimated by the ANAM is generally the most relevant parameter with regard to the paper grade, it is interesting to note that this parameter tends to increase with the paper grade under our experimental conditions. That is to say that the surface morphology is more chaotic for a fine grade paper. It must be pointed out that this conclusion results from a statistical approach. Indeed, each point on Fig. 2 represents the average value of thirty measurements ensuring a significant level of reliability.

3.2. Relevance of surface parameters with regard to surface brightness level

It can clearly be seen on Fig. 2 that: a) the brightness level tends to increase with paper grade for all ground materials, b) the brightness level presents a better linear correlation with Δ_{ANAM} than with the commonly used parameters R_a, R_q and L_{ac}.

The relevance of the fractal dimension with regard to the surface brightness level is particularly confirmed by the analysis of the statistical index of performance P estimated even if one hundred or so surface roughness parameters are considered. Fig. 5 is a typical graph which presents the P values of these parameters in the case of the low carbon steel. The information about the ranking of the relevant parameters of this study is summarized in Table III for all ground materials. The results show that commonly used parameters R_a, R_q are significantly and similarly relevant whereas L_{ac} is by far the least relevant. Once again, the most relevant parameter is the fractal dimension estimated by the ANAM. Except for aluminum (2nd position), this parameter always ranks first position.

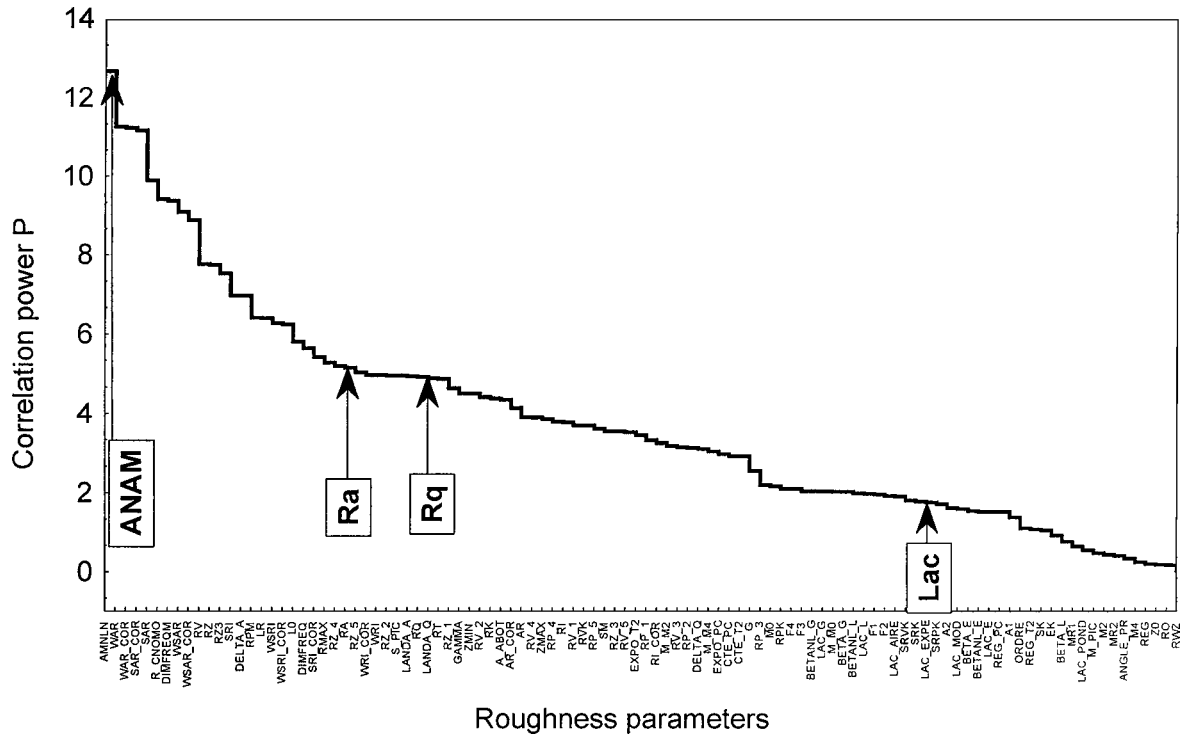

Figure 5 Results of the Bootstrap linear correlation analysis for the ground low carbon steel Fe-0.05%C. Relative roughness parameter ranking according to the value of the statistical index of performance P. The straight dotted line represents the critical value of P under which the surface roughness parameter can be considered as not relevant.

TABLE III Ranking of the relevant parameters of this study with regards to the brightness for all tested materials according to the statistical index of performance P (Bootstrap Linear Correlation Analysis)

Parameters	Al	Cu	Fe-0.05%C	Sn-5%Sb
R_a	18	13	25	14
R_q (σ)	16	19	32	8
LAC_EXPE (L_{ac})	68	87	82	70
DIMFREQ (Δ_s)	59	49	20	65
ANAMLN (Δ_{ANAM})	2	1	1	1

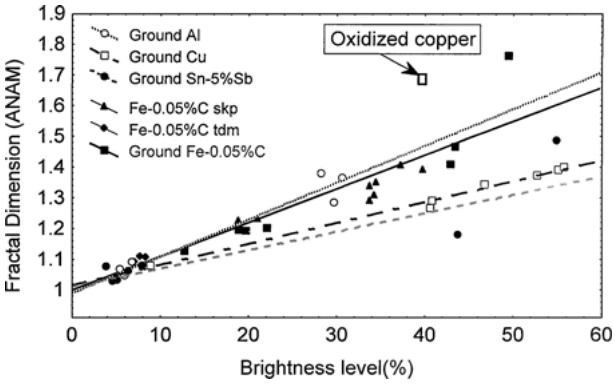

Figure 6 Correlation between surface brightness level and fractal dimension estimated by the ANAM for all materials. Linear regression can be plotted for all materials and whatever the surface damage process (grinding or cold rolling at different roughness levels; the notations SKP and TDM means that the measurements were carried out on the samples taken after the skin pass operation and after the tandem operation respectively) for the industrial low carbon steel Fe-0.05%C. For copper, the aberrant point probably due to oxidation was not taken into consideration for the linear regression calculation.

A linear correlation of brightness level with fractal dimension can be observed in Fig. 6 both for all ground materials and in the case of the industrial cold rolled low carbon steel. Whatever the material, the brightness level tends to increase with the fractal dimension that is to say when the surface morphology becomes more chaotic. Moreover, the slope of the linear regression seems to depend only on the material investigated. It can be concluded that, for a given material, the brightness level depends only on the surface morphology. Nevertheless, one point does not fit with the linear regression associated with the other ones for copper. This point corresponds to blue-colored samples ground at grade 4000. This color, characteristic of an oxidation phenomenon that took place during the grinding process, might sufficiently modify the surface brightness level to introduce an aberrant point in the linear regression calculation. This means that the surface chemistry can probably also play a major role in the surface brightness level in certain cases.

For the low carbon steel, it is very interesting to note that the points associated with the cold rolled samples fits very well with the linear regression associated with those of the ground samples. This means that, whatever the damage (by grinding or cold rolling at different levels of roughness), the fractal dimension can be considered as a relevant parameter to describe the surface morphology and the relationships with the brightness level.

4. Discussion

The statistical results of this study show that the fractal dimension calculated by the ANAM seems to be more appropriate than the commonly used amplitude and frequency surface parameters: a) to describe the machined surface morphology related to an abrasive wear damage by grinding b) to correlate the machined surface morphology obtained by grinding or cold-rolling with the surface's brightness level using a white light beam. Indeed, this surface's roughness parameter nearly always ranks first position.

The fact that the fractal dimension is the most relevant parameter with regard to the paper grade and the surface brightness level probably means that grinding and rolling induce a fractal surface morphology. This result is in agreement with numerous authors' works on different machined surface profiles [26–40].

4.1. Description of machined surface morphologies produced by grinding

It can be intuitively predicted that, whatever the material, the finer the grain size of the grinding paper, the smaller the values of roughness parameters such as R_a, R_q and R_t but also the higher the number of peaks per inch N_p recorded on a profile for a given tracing length. Such a prediction is confirmed on Fig. 2 looking at the evolution of the number of peaks per inch N_p versus paper grade for all ground materials. This increase in the number of peaks per inch N_p indicates that the random surface obtained by grinding becomes more chaotic with higher paper grade. Hence it is no surprise that the finer the grain size, the higher the estimated fractal dimension for a given material. It can also be seen on Fig. 2 that, whatever the paper grade, the surface is more chaotic (the higher is the number of peaks per inch) for hard materials than for soft ones. This result is in agreement with micrographic observations showing that scratches are deeper and less numerous for soft materials than for hard ones under similar grinding conditions.

4.2. Relationship between machined surface morphologies and optical waves

Numerous models on the relation between surface morphology and optical waves are derived from Beckmann's and Spizzichino's pioneering work [6]. By far the largest numbers of these models are based on the Kirchhoff approximation of the boundary conditions, which are required to evaluate the Helmholtz integral. Considering these approximations for perfectly conducting rough surfaces generated by random processes (such surfaces can be described by their Gaussian statistical distributions and correlation function), Beckmann derived the following formula from the calculation of the Helmholtz integral [6]:

$$I/I_0 = \exp\left(-\left(\frac{4\pi R_q \cos\theta}{\lambda}\right)^2\right) + \frac{\lambda^2 L_{ac}^2}{16\pi A R_q^2 \cos^2\theta} \quad (4)$$

where I/I_0 represents the ratio of the scattered intensity in the direction of specular reflection by the intensity of the incident radiation, γ the wavelength, θ the incident angle, A the scattering zone area, R_q the root-mean squared roughness and L_{ac} the correlation length of the surface.

The two terms of this relation correspond respectively to the specular and the diffuse components of the scattered light; the former dominates for smooth surfaces while the latter dominates for rough surfaces. It must be noted that the domain of applicability of this relation has limits according to the value of the ratio R_q/λ as mentioned by Vorburger *et al.* [41, 42]. When this ratio exceeds a threshold value of 0.3 for different rough metallic surfaces, these authors found that the diffuse component dominates but the flux is fairly insensitive to changes in roughness. This implicitly means that no strong correlation could be found between R_q and the reflected intensity in this case.

In fact, most of the models derived from Beckmann's express the scattered intensity of an optical wave as a function of the scattering angle, the electromagnetic properties of the studied material, the wavelength and commonly used surface parameters such as R_q and L_{ac}. It must be pointed out that these models have been developed for periodically (sinusoidal or saw-tooth profiles) and random surface roughness.' However, wave interactions with fractal rough surfaces have also been studied more recently [43–48].

Several authors also used Kirchhoff approximations in their work to describe the optical properties of fractal structures. For example, Jaggard [43] developed a method to characterize the fractal dimension of a surface remotely using the Kirchhoff method to calculate the distribution of the scattered energy as a function of scattering angle for different values of surface roughness. He showed that the surface roughness increases and more of the scattered energy is diverted from the specular direction as the fractal dimension of the surface increases. In the same way, Sheppard [44] predicts for a rough two-dimensional surface with stationary statistics and a normal distribution of heights that the scattering varies like $c/h^{2(3-\Delta s)}$. In the previous formula, Δ_s is the fractal dimension of the surface that can vary between 2 and 3 ($\Delta_s = 2$ corresponds to an ideally smooth surface and $\Delta_s = 3$ corresponds to a rough surface), c and h can be regarded respectively as normalized correlation length (by the radial spatial frequency) and normalized root mean-square surface height (by the axial spatial frequency). However, this theoretical work by Sheppard was not confirmed by any experimental evidence.

Moreover, as outlined by Jakeman [45], though continuous, a Gaussian random fractal surface is not differentiable. Thus, the notion of tangent plane necessary to estimate the Helmholtz integral (the scattered intensity) within Kirchhoff approximations does not exist anymore for a fractal representation of surface roughness [47]. This conclusion is in agreement with Botet *et al.* [48] who claim that neither the Rayleigh perturbation approximation nor the Kirchhoff approach can be applied to describe the optical properties of a fractal self-affine structure.

In their work, Botet *et al.* [48] adopted the microscopic "discrete–dipole approximation" (DDA) initially suggested by Purcell and Pennypacker [49] and lately developed by Draine [50] to calculate the optical response from an object having an arbitrary shape. They numerically generated a surface with self-affine fractal structure, similar to that of a cold deposited metal, treating it as a collection of N linear polarizable particles for which the linear size is assumed to be much smaller than the wavelength. They showed that for a self-affine fractal surface, the spatial distribution of the local field (or the scattered intensity) is extremely non homogeneous and that the non-linear optical responses are dramatically enhanced compared to those of smooth interfaces.

These result as well as our experimental data lead to the conclusion that a great attention has to be paid to the surface morphology with respect to the wavelength before applying any optical theory. However, the main challenge consists in describing thoroughly the geometry of the surface asperities. To study the interactions between surface morphology and optical waves, numerous authors apply the Kirchhoff approximations in which the geometry of an asperity is described by its curvature radius r_{ci} that is assumed to be higher than the wavelength λ [6, 47, 51–53].

To estimate the curvature radius r_{ci} of an asperity, Nowicki [54] mentioned a method that leads to the following formula:

$$r_{ci} = \frac{l_{xi}^2}{8 l_y} \quad \text{with } l_y = \alpha R_t \text{ and } \alpha = 0.05 \text{ or } 0.1 \quad (5)$$

where l_{xi} and l_y are defined on Fig. 7a and R_t is the maximal range amplitude of the profile.

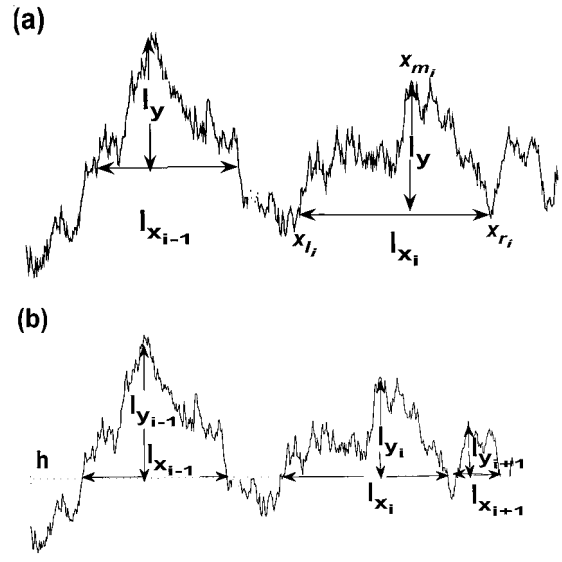

Figure 7 Graphic vizualisation of the calculation of the curvature radii of asperities on a stochastic profile using: (a) the Nowicki method where the level l_y is fixed ($l_y = 0.1R_t$ or $l_y = 0.05R_t$) and (b) the new method proposed in this study in which a set of pairs (l_{xi}, l_{yi}) can be determined at each level h.

This method consists in determining the radius of a circle that passes in the three points x_i, x_r and x_m assuming $l_y \ll l_x$. However, the choice of the threshold value of α (0.05 or 0.1) to estimate l_y is arbitrary and does not have any theoretical justification. Moreover, this method of calculation of r_{ci} does not make sense as far as fractal profiles are concerned. Indeed, for a fractal profile, the radius curvature r_{ci} depends on the observation scale related to the value of α which is fixed in the above method.

As the relevance of fractal dimension to describe the morphology of machined surfaces is outlined both in literature [26–40] and in this study, a new method is proposed to calculate the radius curvature r_{ci} of an asperity as a function of the observation scale. The different steps of this new method are listed below:

- A horizontal line is fixed at a level h crossing the profile to obtain a set of l_{xi} values as defined on Fig. 7b;
- For each l_{xi} value, the related l_{yi} value that characterizes the local maximum height is computed;
- Then, for each "peak," the calculation of r_{ci} is computed using Equation 5. These operations are repeated for each element of the set of l_{xi} values;
- Another horizontal height is chosen and steps a to c are repeated. On the whole, one hundred equally spaced intercept lines covering the whole amplitude height range of the profile have been studied.

This method has first been applied on different uniformly Hölderian and anti Hölderian simulated stochastic fractal profiles whose fractal dimensions are respectively equal to 1, 1.5 and 1.8. For each value of the fractal dimension, one thousand stochastic profiles have been simulated and Fig. 8 clearly presents a linear evolution of $\log r_c$ versus $\log l_x$. In each case, the calculated slope is equal to the fractal dimension and it can thus be written:

$$\log r_c = b + \Delta \log l_x \tag{6}$$

Moreover, it was proved [16] that for all non constant continuous functions f defined on $[a, b]$ which are uniformly Hölderian and anti Hölderian that:

$$\text{if } l_x \text{ exists, } \Delta(f, a, b) = \lim_{l_x \to 0} \sup(\log r_c / \log l_x) \tag{7}$$

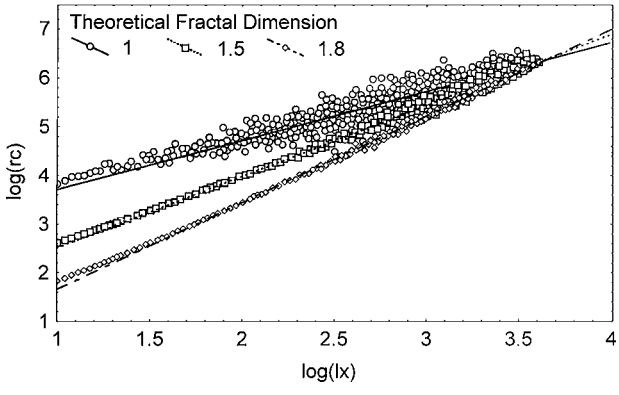

Figure 8 Evolution of $\log r_c$ versus $\log l_x$ for uniformly Hölderian and anti Hölderian simulated stochastic fractal profiles whose theoretical fractal dimensions are respectively equal to 1, 1.5 and 1.8. Considering a great number of profiles (1000 in this case), the slope of each regression line is equal to the fractal dimension.

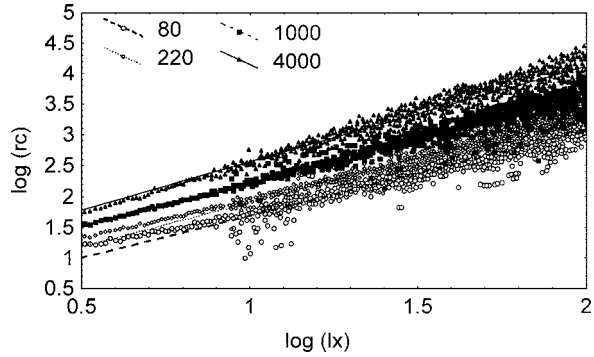

Figure 9 Influence of paper grade on the evolution of $\log r_c$ versus $\log l_x$ for the ground low carbon steel Fe-0.05%C. The linear regression line is plotted for each paper grade.

As the profiles recorded from machined surfaces obtained by grinding have these properties [16], the method described above has been applied to all the experimental profiles of this study. Fig. 9 represents the plots of $\log r_c$ versus $\log l_x$ in the case of the ground low carbon steel for several paper grade. Each plot represents more than 3000000 pairs of values (l_{xi}, r_{ci}) for which the mean of the r_{ci} values has been computed for l_x steps of 0.1 μm. This figure shows that a linear correlation is observed whatever the paper grade. However, the estimation of the fractal dimension of these experimental profiles is more precise by using ANAM which averages the experimental data using a double integral [22] rather than Equation 6. Indeed, only thirty experimental profiles have been recorded for each paper grade whereas Equation 6 has been determined from the analysis of one thousand profiles of simulated stochastic fractal profiles. Unfortunately, it is not possible to consider experimentally such a high number of profiles only because it is time consuming. It must be outlined that the same tendencies are revealed from the analysis of the experimental data of the other studied materials.

Looking at Fig. 9, it is clear that the curvature radius increases as the observation scale increases. Secondly, for a fixed observation scale l_x, it could be observed that the higher the paper grade, the higher the curvature radius. As statistically proved by the experimental results, the higher the fractal dimension, the higher the brightness level. According to Equation 6, the slope of the log-log plot is given by the fractal dimension of the profile and then the higher the fractal dimension, the higher the curvature radius.

For two profiles P_1 and P_2 such as $\Delta_1 > \Delta_2$, we can infer from Equation 6 that there exists a critical length l_x^c given by $\log l_x^c = (b_2 - b_1)/(\Delta_1 - \Delta_2)$. Below l_x^c the average curvature radius of the asperities r_c (if it exists meaning that $l_y \ll l_x$) is lower for profile P_1 than for profile P_2 whereas the average curvature radius of the asperities of the profile having the higher fractal dimension is higher above l_x^c. This critical length l_x^c depends on the b_1 and b_2 values of Equation 6.

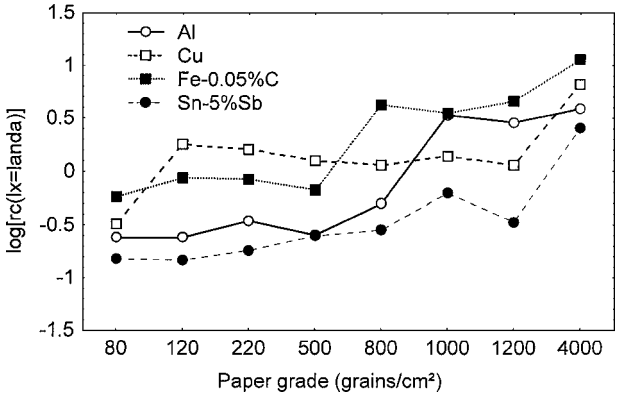

Figure 10 Values of the average curvature radius (in log) corresponding to an ≪electromagnetic yardstick≫ $l_x^\lambda = \gamma = 0.6\ \mu$m for the different ground materials and paper grades.

The definition of r_{ci} for a fractal profile is meaningful only at the observation scale l_x of the asperities. However, the choice of the observation scale has to be made according to the studied physical phenomenon. In the optical case, an electromagnetic characteristic length can be considered as done by Jaggard [41] who chooses the wavelength of the radiation as an ≪electromagnetic yardstick≫ noted l_x^λ in this study. Fig. 10 represents the values of the average curvature radius for each paper grade and materials for $l_x^\lambda = \lambda = 0.6\ \mu$m (the average wavelength of a white light beam). In each case, the coefficients b and Δ were calculated using the linear least square method. Compared to the equivalent graphical representation of brightness level (Fig. 2), the evolution of the average curvature radius follows the same tendencies with the paper grader as the brightness level. For a given material, the higher the fractal dimension, the higher the average curvature radius of the surface asperities and the higher the brightness level. This clearly means that a more chaotic surface could be seen as smoother by the incident radiation if $\lambda \gg l_x^c$ which is the case in our study.

To summarize, the method proposed in this study to calculate the curvature radius of the asperities explains the increase in the brightness level with the fractal dimension of each investigated material. Some theoretical aspects are still under study so as to precise the relationships between the optical notion of the Airy disk radius and the average curvature radius of the asperities of a fractal surface.

5. Conclusion

A new methodology is proposed to characterize the interactions between machined surface topography and an optical wave. The aim of this methodology is to provide a quantitative determination of the relative relevance of one hundred or so roughness parameters through the calculation of statistical indexes of performance. These indexes were estimated combining the variance analysis and the linear correlation analysis with the recent and powerful Bootstrap theory. The final ranking gives the most appropriate roughness parameter for the characterization of the surface morphology.

Using a specific program developed for this study, it was shown that: a) the commonly used roughness parameters are not the most relevant ones to describe both the morphology of machined surfaces obtained by grinding or cold rolling and their relationships with their brightness level, b) except in one case, the fractal dimension estimated by the ANAM is the most relevant parameter, c) the brightness level increases linearly with the fractal dimension of the machined surface.

It must be outlined that several measures have been taken to emphasize the reliability of the experimental results. Firstly, four metallic materials with different microstructure, mechanical and optical properties were considered. Secondly, a high number of measurements were performed and, thirdly, it was verified that measurement artifacts did not influence the statistical results. All the results of this study seems to indicate that grinding and cold rolling induces a fractal surface morphology that can be described by its fractal dimension; a roughness parameter taking into consideration both amplitude and frequency variations. Thus, this surface roughness parameter should be considered as a privileged candidate in models showing the interactions between the morphology of machined surfaces and optical waves.

The methodology proposed in this study can be a useful tool to determine which roughness parameter evolution must be analyzed in a quality control phase in order to control the fabrication process of manufactured objects in industrial environments. It must also be emphasized that this methodology, developed here to understand more precisely the relationships between surface topography and an optical wave, can be generalized whatever the considered physical phenomenon.

Acknowledgment

The authors want to thank the anonymous referee to have brought to their knowledge the existence of some relevant references related to the optical field. The authors also thank V. Hague for the language corrections of the original manuscript.

Appendix A: Variance analysis

The variance analysis is used to estimate if the difference between means is significant or not using the Null Hypothesis.

First, it should be remembered that for a given sample size, s, the variance is calculated by dividing the sum of squared deviations of scores from the mean by $s - 1$. The heart of the variance analysis is that the total deviation (the sum of squared deviations from the mean) can be partitioned into two component deviations: one based on the deviation of any score from its treatment mean (within-group deviation) and the other based on the deviation of the treatment mean from the grand mean (treatment-group deviation). The first component reflects the unavoidable effects of experimental error alone whereas the second one reflects both the effects of treatment and experimental error.

Since the sum of squares is not directly manageable because of the number of deviations which

affects it, the mean square or variance is calculated dividing the sum of squares by the number of degrees of freedom. Then, a ratio of treatment-group variability (called Mean Square Effect) relative to the within-group variability (called Mean Square Error) is introduced. This ratio called Treatment Index and noted F will be used to evaluate the Null Hypothesis which states that the two population treatment means considered are equal, that is, the complete absence of treatment effects.

The Treatment Index F should be approximately equal to one when treatment effects are completely absent and should be higher than one when they are present. However, because of the chance factors operating in any experiment, the estimated Treatment Index F must equal or exceed a critical value to reject the Null Hypothesis and conclude that some treatment effect affects the population mean. This critical value noted $F^{5\%}$ is the value of the Treatment Index that will be exceeded by chance only 5 percent of the time when the Null Hypothesis is true. If the estimated value of F is smaller than this critical value $F^{5\%}$ the Null Hypothesis cannot be rejected and the eventual calculated differences between means are best interpreted in term of chance factors.

Appendix B: Bootstrap analysis

Bootstrap theory is due to Efron [17, 18]. The principle of this theory consists in elaborating an empirical Probability Density Function (PDF) of a variable from generated Bootstrap samples (L copy of the surface profiles and random collects on this set). Then from the PDF, it becomes possible to build a statistical test about a given hypothesis. One great advantage of this method is that no restricted hypothesis about the distribution of experimental data has to be supposed and so verified. So, there is no risk that the violation of the assumptions might lead to wrong conclusion.

Let us consider first the original set of experimental data noted $[q^1_{i,j}, q^2_{i,j}, q^3_{i,j}, q^4_{i,j} \cdots, q^{n_{i,j}}_{i,j}]$ where $q_{i,j}$ is for example a value of a roughness parameter q_i obtained from a sample j and $n_{i,j}$ is the number of measurements. Each element $q^k_{i,j}$ of this set has a probability of $\frac{1}{n_{i,j}}$ to be selected and thus an equivalent configuration $[q^1_{i,j}, q^2_{i,j}, q^2_{i,j}, q^4_{i,j} \cdots, q^{n_{i,j}}_{i,j}]$ could also have been obtained instead of the original configuration taking into consideration only chance factor. In the same way, a probability of $(\frac{1}{n_{i,j}})^{n_{i,j}}$ can be attributed to the configuration: $[q^1_{i,j}, q^1_{i,j}, q^1_{i,j}, q^1_{i,j} \cdots, q^1_{i,j}]$.

Let us consider now $[\hat{q}^1_{i,j}, \hat{q}^2_{i,j}, \hat{q}^3_{i,j}, \hat{q}^4_{i,j} \cdots, \hat{q}^{n_{i,j}}_{i,j}]$ the new Bootstrap sample where $q^k_{i,j}$ is repeated $m^k_{i,j}$ times (thus $m^1_{i,j} + m^2_{i,j} + \cdots + m^k_{i,j} = n_{i,j}$). The probability that $q^k_{i,j}$ has to be repeated $m^k_{i,j}$ times among the $n_{i,j}$ selections, is given by $Pr_{i,j}(m^1_{i,j}, m^2_{i,j}, \cdots, m^k_{i,j}) = \frac{n_{i,j}}{n^{n_{i,j}}_{i,j} m^1_{i,j}!, m^2_{i,j}!, \cdots, m^k_{i,j}!}$. The non probability-repetition of the Bootstrap sample is given by $P_{i,j} = \frac{n_{i,j}!}{n^{n_{i,j}}_{i,j}}$. This parameter is important because it indicates the probability that the Bootstrap simulation gives a discontinuous distribution. To simulate N Bootstrap samples, two principal steps must be considered:

1) From the initial set of data, for each population $q_{i,j}$, $n_{i,j}$ samples are pulled at random according to a uniform law. The operation consists in simulating $n_{i,j}$ integer random numbers $a_p(p = 1, 2, \cdots, n_{i,j})$ belonging to the interval $[1 \cdots n_{i,j}]$ and then to extract a Bootstrap sample $\hat{q}^1_{i,j} = q^{a_1}_{i,j}, \cdots, \hat{q}^{n_{i,j}}_{i,j} = q^{a_{n_{i,j}}}_{i,j}$.

2) This operation is repeated N times and we will call ${}^l\hat{q}^k_{i,j}$ the kth measurement from the lth Bootstrap simulation of the parameter q_i belonging to the jth sample.

References

1. E. S. ZANORIA, T. R. WATKINS, K. BREDER, L. RIESTER, M. BASHKANSKY, J. REINTJES, J. G. SUN, W. A. ELLINGSON and P. J. BLAU, *J. of Mater. Eng. and Perform.* **7** (1998) 533.
2. F. BERNY, *Mécanique* **311/312** (1975) 23.
3. J. P. GOEDGEBUER and J. C. VIÉNOT, *Bulletin BNM* **44** (1981) 3.
4. U. PERSSON, *Wear* **160** (1993) 221.
5. J. C. LE BOSSE, G. HANSALI, J. LOPEZ and J. C. DUMAS, *ibid.* **224** (1999) 236.
6. P. BECKMANN and A. SPIZZICHINO, "The Scattering of Electromagnetic Waves from Rough Surfaces" (Pergamon Press, London, 1963).
7. B. MANDELBROT, *Science* (1967) 636.
8. *Idem.*, "Les Objets Fractals: Forme, Hasard et Dimension" (Flammarion, Paris, 1975).
9. *Idem.*, "The Fractal Geometry of Nature" (W. H. Freeman and Company, New York, 1983).
10. A. LE MEHAUTE, "Les Géométries Fractales" (Hermés, Paris, 1990).
11. J. F. GOUYET, "Physique et Strutures Fractales" (Masson, Paris, 1992).
12. J. J. GAGNEPAIN and C. ROCQUES-CARMES, *Wear* **109** (1986) 119.
13. A. MAJUMDAR and C. L. TIEN, *ibid.* **136** (1990) 313.
14. S. CHESTER, H. C. WANG and G. KASPER, *Solid State Technology* **34** (1991) 73.
15. SHI WEI MIN, S. P. LIM and K. S. LEE, *Optics and Laser Technology* **27** (1995) 331.
16. M. BIGERELLE, Phd thesis, Ecol Nationale Supérieure d'Arts et Métiers, Lille, France, 1999.
17. B. EFRON, *Ann. Statis.* **7** (1979) 1.
18. B. EFRON and R. J. TIBSHIRANI, "An Introduction to the Bootstrap" (Chapman and Hall, London, 1993).
19. P. HALL, "The Bootstrap and the Edgeworth Expansion" (Springer-Verlag, Berlin, 1992).
20. J. SHAO and D. TU, "The Jacknife and the Bootstrap" (Springer-Verlag, Berlin, 1996).
21. G. KEPPEL and W. H. SAUFFLEY, "Introduction to Design and Analysis" (W. H. Freeman and Company, New York, 1980).
22. M. BIGERELLE and A. IOST, *C. R. Acad. Sci. Paris* **323** Série II b (1996) 669.
23. M. BIGERELLE and A. IOST, *Computer and Mathematics with Applications* **42** (2001) 241.
24. B. DUBUC, J. F. QUINIOU, C. ROQUES-CARNES, C. TRICOT and S. W. ZUCKER, *Phys. Rev.* A **39** (1989) 1500.
25. ANSI B46.1-1995, Specification for Surface Texture (Surface Roughness, Waviness and Lay) ASME, New York.
26. C. A. BROWN and G. SAVARY, *Wear* **141** (1991) 211.
27. C. A. BROWN, P. D. CHARLES, W. A. JOHNSEN and S. CHESTERS, *ibid.* **161** (1993) 61.
28. G. SHIRONG and C. GOUAN, *ibid.* **231** (1999) 249.
29. T. R. THOMAS, B. G. ROSÉN and N. AMINI, *ibid.* **232** (1999) 41.
30. M. S. BOBJI, K. VENKATESH and S. K. BISWAS, *J. of Tribology* **121** (1999) 746.
31. C. G. LI, S. DONG and G. X. ZHANG, *ibid.* **232** (1999) 76.
32. F. PLOURABOUÉ and M. BOEHM, *Tribology International* **32** (1999) 45.
33. H. PAWELSKI, *Steel Research* **67** (1996) 144.

34. S. GANTI and B. BHUSHAN, *Wear* **180** (1995) 17.
35. E. DOEGE, B. LAACKMAN and B. KISCHNICK, *Annals of the CIRP* **44** (1995) 197.
36. L. HE and J. ZHU, *Wear* **208** (1997) 17.
37. C. A. BROWN, W. A. JOHNSEN and R. M. BUTLAND, *Annals of the CIRP* **45** (1996) 515.
38. T. JOSSANG and J. FEDER, *Physica Scripta* **44** (1992) 9.
39. C. TRICOT, P. FERLAND and G. BARAN, *Wear* **172** (1994) 127.
40. F. F. LING, *ibid.* **136** (1990) 141.
41. T. V. VORBURGER, E. MARX and T. R. LETTIERI, *Appl. Opt.* **32** (1993) 3401.
42. T. V. VORBURGER and E. C. TEAGUE, *Prec. Eng.* **3** (1981) 61.
43. D. L. JAGGARD, in "Fractals in Engineering," edited by J. L. Vehel, E. Lutton and C. Tricot (Springer-Verlag, Berlin, 1997) p. 204.
44. C. J. R. SHEPPARD, *Opt. Comm.* **122** (1996) 178.
45. E. JAKEMAN, in "Waves in Random Media," edited by J. C. Dainty and D. Maystre (An Institute of Physics Journal, 1991) p. 1, 109.
46. *Idem., J. Phys.* A **15** (1982) L55.
47. P. CALLET, in "Couleur-Lumiére Couleur-Matiére: Interaction Lumiére-Matiére et Synthése d'Images," Diderot Editeur, Arts et Sciences Paris, 1998.
48. R. BOTET, E. Y. POLIAKOV, V. M. SHALAEV and V. A. MARKEL, in "Fractals in Engineering," edited by J. L. Vehel, E. Lutton and C. Tricot (Springer Verlag, Berlin, 1997) p. 237.
49. E. M. PURCELL and C. R. PENNYPACKER, *Astrophys J.* (1973) 186 cited by [44].
50. B. T. DRAINE, *Astrophys. J.* (1998) 333 cited by [44].
51. J. C. DAINTY, N. C. BRUCE and A. J. SANT, in "Waves in Random Media," edited by J. C. Dainty and D. Maystre (An Institute of Physics Journal, 1991) p. 1, 29.
52. A. ISHIMARU, S. C. JEI, P. PHU and K. YOSHITOMI, in "Waves in Random Media," edited by J. C. Dainty and D. Maystre (An Institute of Physics Journal, 1991) p. 1, 91.
53. D. L. JAGGARD and X. SUN, *J. Opt. Soc.* A **7** (1990) 1131.
54. B. NOWICKI, *Wear* **102** (1985) 161.

Received 18 September 2001
and accepted 16 January 2003